ELSEVIER

14 December 1998

PHYSICS LETTERS A

Physics Letters A 249 (1998) 495–500

Oscillation frequencies for a Bose condensate in a triaxial magnetic trap

E. Cerboneschi [a], R. Mannella [a], E. Arimondo [a], L. Salasnich [b]

[a] *Istituto Nazionale per la Fisica della Materia, Unità di Pisa, Dipartimento di Fisica, Università di Pisa, Via Buonarroti, I-56127 Pisa, Italy*

[b] *Istituto Nazionale per la Fisica della Materia, Unità di Milano, Dipartimento di Fisica, Università di Milano, Via Celoria 16, I-20133 Milan, Italy*

Received 10 September 1998; accepted for publication 18 September 1998
Communicated by V.M. Agranovich

Abstract

We investigate the dynamics of a Bose condensate, interacting with either repulsive or attractive forces, confined in a fully anisotropic harmonic potential. The $(3+1)$-dimensional Gross–Pitaevskii equation is integrated numerically to derive the collective excitation frequencies, showing a good agreement with those calculated with a variational technique. © 1998 Elsevier Science B.V.

PACS: 03.75.Fi; 05.30.Jp; 32.80.Pj

In Bose–Einstein condensation, an atomic sample confined within a magnetic trap is brought into a new state of matter, described by a single macroscopic quantum-mechanical wave function. The condensation process starts from a sample in vapour phase, and proceeds through applications of laser cooling and evaporative cooling [1–3]. The condensate may contain between one thousand and a few million atoms. Around zero temperature or when the non-condensate may be neglected, the description of the macroscopic wave function is given by the nonlinear Gross–Pitaevskii equation [4]. Recently, much attention within the Bose–Einstein condensation community has been concentrated on the excitation of condensate oscillations through a modulation of the confining potential produced by the magnetic trap [5–7]. The experimental and theoretical investigation of the condensate oscillation eigenmodes has provided important information on the condensate. The validity of the theoretical treatments has been tested, the atom coupling has been investigated in the different regimes, the processes responsible for the damping of the eigenmodes have been determined.

In this work, we examine theoretically the condensate eigenmodes in a magnetic trap configuration leading to a very complex dynamics. Most previous analyses examined magnetic traps having either spherical or cylindrical symmetries, where the oscillation eigenmodes are determined by the trap symmetry. A different trap geometry, with different elastic constants along the three orthogonal axes, has been investigated in an experiment on sodium atoms, based on a triaxial TOP trap [8]. In this Letter we examine, for the first time, the collective frequencies associated to that magnetic trap. The calculation of the oscillation collective frequencies requires solving the Gross–Pitaevskii

PII S0375-9601(98)00732-4

equation (GPE) in order to determine the condensate spatial distribution in the ground state. Such a solution makes it possible also to investigate the modification of the condensate distribution following a modification of the magnetic trap geometry, for instance as a consequence of an oscillation of the trap confining potential. The GPE is here analyzed using the variational method based on the Gaussian ansatz for the shape of the macroscopic wave function of the condensate, applied to the study of the nonlinear Schrödinger equation in nonlinear optical wave propagation [9] and for the investigation of the Bose–Einstein condensate in cylindrical [10] and spherical [11] symmetry traps. This variational approach is here extended to the triaxial magnetic trap. We derive the low-energy excitation spectrum of the collective motion for both positive and negative scattering lengths, as a function of the atom–atom interaction strength. Our analysis is valid for the whole range of coupling strengths, and, in the limit of large coupling, we recover the predictions of the hydrodynamic approach in the Thomas–Fermi approximation [4]. We have also solved numerically the $(3+1)$-dimensional GPE, and derived the condensate mode frequencies examining the oscillation frequencies excited in the temporal evolution of the condensate wavefunction. The agreement between the collective mode frequencies calculated with the approximate variational technique and those arising from the exact numerical integration is within a few percent.

The macroscopic condensate wave function ψ, describing an average number N of interacting bosons trapped in an external potential V at zero temperature, obeys the time-dependent GPE

$$i\hbar\frac{\partial}{\partial t}\psi(\boldsymbol{r},t) = \left(-\frac{\hbar^2\nabla^2}{2m} + V(\boldsymbol{r}) + g|\psi(\boldsymbol{r},t)|^2\right) \times\psi(\boldsymbol{r},t)\,, \tag{1}$$

where m is the mass of the atom and the coupling constant g is given by $g = 4\pi\hbar^2 a/m$, with a the s-wave scattering length. The time-dependent GPE can be derived by minimizing the action $S = \int \mathcal{L}\,\mathrm{d}^3\boldsymbol{r}\,\mathrm{d}t$ related to the Lagrangian density

$$\mathcal{L} = i\hbar\psi^*\frac{\partial\psi}{\partial t} = \frac{\hbar^2}{2m}\nabla\psi^*\cdot\nabla\psi - V(\boldsymbol{r})|\psi|^2 - \tfrac{1}{2}g|\psi|^4\,. \tag{2}$$

We consider a triaxially asymmetric harmonic trapping potential of the form

$$V(\boldsymbol{r}) = \tfrac{1}{2}m\omega_0^2(\lambda_1^2x^2 + \lambda_2^2y^2 + \lambda_3^2z^2)\,, \tag{3}$$

where the adimensional constants λ_i^2 $(i = 1,2,3)$ are proportional to the spring constants of the potential along the three axes.

Minimizing the action S within a Gaussian trial function makes it possible to obtain, for the condensate wave function, approximate solutions which can be derived, to a large extent, analytically [9–11]. In the limit of weak interatomic coupling, i.e., small boson number and small scattering length, the choice of a Gaussian shape for the condensate is well justified because it describes the exact solution of the linear Schrödinger equation with harmonic potential. For the description of the collective dynamics of a Bose–Einstein condensate trapped in a spherically or cylindrically symmetric potential, it has already been shown that the variational technique based on Gaussian trial functions leads to reliable results even in the large condensate number limit [10]. We take a trial function of the form

$$\psi(\boldsymbol{r},t) = N^{1/2}\left(\frac{1}{\pi^3\tilde{\sigma}_1^2(t)\,\tilde{\sigma}_2^2(t)\,\tilde{\sigma}_3^2(t)}\right)^{1/4} \times\prod_{i=1,2,3}\exp\left(-\frac{x_i^2}{2\tilde{\sigma}_i^2(t)} + i\beta_i(t)\,x_i^2\right), \tag{4}$$

with $(x_1,x_2,x_3) \equiv (x,y,z)$, where $\tilde{\sigma}_i$ and β_i are time-dependent variational parameters and the wave function is normalized to the number N of bosons. Please note that, in order to describe the time evolution of the variational function, the phase factor $i\beta_i(t)x_i^2$ is needed [9].

From the Euler–Lagrange equations, the following equations of motions for the variational parameters are derived:

$$\ddot{\tilde{\sigma}}_i(t) + \lambda_i^2\omega_0^2\tilde{\sigma}_i(t) = \frac{\hbar^2}{m^2\tilde{\sigma}_i^3(t)} + \sqrt{\frac{2}{\pi}}\,\frac{a\hbar^2N}{m^2\tilde{\sigma}_i(t)\,\tilde{\sigma}_1(t)\,\tilde{\sigma}_2(t)\,\tilde{\sigma}_3(t)}\,, \tag{5a}$$

$$\beta_i(t) = -\frac{m\dot{\tilde{\sigma}}_i(t)}{2\hbar^2\tilde{\sigma}_i(t)}\,, \tag{5b}$$

with $i = 1,2,3$. From Eq. (5b), we observe that the time dependence of β_i is determined by that of $\tilde{\sigma}_i$. Introducing the adimensional parameters $\tau = \omega_0 t$ and $\sigma_i = \tilde{\sigma}_i/a_0$, where $a_0 = (\hbar/m\omega_0)^{1/2}$ is the harmonic oscillator length, Eq. (5a) becomes

$$\frac{d^2}{d\tau^2}\sigma_i + \lambda_i^2\sigma_i = \frac{1}{\sigma_i^3} + \frac{\tilde{g}}{\sigma_i\sigma_1\sigma_2\sigma_3}\,. \tag{6}$$

Here, we have defined the coupling strength $\tilde{g} = (2/\pi)^{1/2}Na/a_0$, proportional to the condensate number N and the scattering length a, which determines the atom–atom interaction compared to the bare trapping potential. Eqs. (6), with $i = 1,2,3$, represent a set of three nonlinearly coupled ordinary differential equations describing the time evolution of the widths of the condensate along each direction[1]: formally, they correspond to the classical equations of motion for a particle with coordinates σ_i and total energy $E = T + U$, with

$$T = \tfrac{1}{2}(\dot{\sigma}_1^2 + \dot{\sigma}_2^2 + \dot{\sigma}_3^2)\,, \tag{7a}$$

$$U = \tfrac{1}{2}(\lambda_1^2\sigma_1^2 + \lambda_2^2\sigma_2^2 + \lambda_3^2\sigma_3^2) + \tfrac{1}{2}\left(\frac{1}{\sigma_1^2} + \frac{1}{\sigma_2^2} + \frac{1}{\sigma_3^2}\right) + \tilde{g}\frac{1}{\sigma_1\sigma_2\sigma_3}\,, \tag{7b}$$

where the dots indicate the derivative with respect to τ. T plays the role of kinetic energy and the three terms in U, arising from the harmonic trapping potential, the kinetic pressure, and the atom–atom interaction, respectively, represent an effective potential energy.

The frequencies of the low-energy excitations of the condensate correspond to the small oscillations of the variables σ's around the equilibrium point, given by the minimum of the effective potential energy U in Eq. (7b). First, we find the equilibrium point solving the equations

$$\lambda_i^2\sigma_i^4 - \tilde{g}\frac{\sigma_i}{\sigma_j\sigma_k} = 1\,, \tag{8}$$

with i, j, k ranging from 1 to 3 and different from each other.

[1] Eqs. (6) reduce, in the limit of large coupling strength, to those derived from the hydrodynamic equations in the Thomas–Fermi approximation. See, for instance, Eqs. (97) of Ref. [4]. Other derivations of the same equations, for large coupling strength, are given in Ref. [12].

Then, after a second-order Taylor expansion of U around the minimum, we linearize Eqs. (6) around the stationary point. The calculation of the normal mode frequencies for the motion of the condensate is reduced to an eigenvalue problem for the matrix Λ, given by

$$\Lambda_{ij} = \left.\frac{\partial^2 U}{\partial\sigma_i\partial\sigma_j}\right|_{\boldsymbol{\sigma}=\boldsymbol{\sigma}^0}\,, \tag{9}$$

where $\boldsymbol{\sigma}^0 = (\sigma_1^0, \sigma_2^0, \sigma_3^0)$ stands for the solution of Eq. (8). In the Thomas–Fermi limit, i.e., for $\tilde{g} \gg 1$, the right-hand side in Eq. (8), related to the kinetic pressure, can be neglected and an analytic expression for the equilibrium point is obtained. In this case, the eigenfrequencies ω for the collective motion, in units of ω_0, are given by the solutions of the equation

$$0 = \omega^6 - 3(\lambda_1^2 + \lambda_2^2 + \lambda_3^2)\omega^4 + 8(\lambda_1^2\lambda_2^2 + \lambda_1^2\lambda_3^2 + \lambda_2^2\lambda_3^2)\omega^2 - 20\lambda_1^2\lambda_2^2\lambda_3^2\,. \tag{10}$$

The same equation, obtained within a hydrodynamic approach, is reported in Ref. [4]. In the opposite limit, for $\tilde{g} = 0$, we recover the well-known result $\omega_i = 2\lambda_i$, with $i = 1,2,3$, in units of ω_0, for the normal modes in the non-interacting case.

The numerical integration of the time-dependent GPE, in Eq. (1), was done using a modified split operator technique, adapted to the integration of a Schrödinger equation. We wrote Eq. (1) in the form

$$i\hbar\frac{\partial}{\partial t}\psi(\boldsymbol{r},t) = [H_x(\boldsymbol{r},t) + H_y(\boldsymbol{r},t) + H_z(\boldsymbol{r},t)] \times \psi(\boldsymbol{r},t)\,, \tag{11}$$

where

$$H_i(\boldsymbol{r},t) \equiv -\frac{\hbar^2}{2m}\frac{\partial^2}{\partial x_i^2} + V(x_i) + \tfrac{1}{3}g|\psi(\boldsymbol{r},t)|^2\,. \tag{12}$$

The idea is to split the full Hamiltonian in three sub-Hamiltonians, so that at each time we have to write the Laplacian with respect to one coordinate only, leading to the solution of a tridiagonal system, and to huge savings in computer memory. The splitting is carried out so that the commutators are exact up to the order δ^2 included. Eq. (11) was integrated using the scheme (δ is the integration time step, and $A_i(t) \equiv i\delta H_i(\boldsymbol{r},t)/\hbar$)

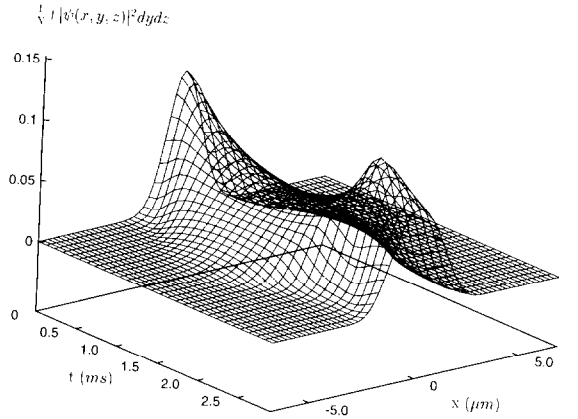

Fig. 1. A typical result of the numerical integration of the GPE: plot of $N^{-1}\int |\psi(\boldsymbol{r},t)|^2\,\mathrm{d}y\,\mathrm{d}z$ versus t and x. We used the Na parameters for the integration (see text), and $\tilde{g} = 3.335$.

$$\psi(\boldsymbol{r},t+\delta) = \frac{1}{1+A_y(t)/2}[1-\tfrac{1}{2}A_x(t)] \times \frac{1}{1+A_z(t)/2}[1-\tfrac{1}{2}A_z(t)] \times \frac{1}{1+A_x(t)/2}[1-\tfrac{1}{2}A_y(t)]\psi(\boldsymbol{r},t)\,. \qquad (13)$$

There is obviously a problem with the nonlinear term $g|\psi(\boldsymbol{r},t)|^2$, because we should really use a ψ somehow averaged over the time step δ, not a ψ evaluated at the beginning of the time step. To circumvent this problem, we used a sort of predictor–corrector step. Each integration step is really done in two times: going from the time t to the time $t+\delta$, the first time we used $\psi(\boldsymbol{r},t)$ in the nonlinear term, obtaining a "predicted" $\tilde{\psi}(\boldsymbol{r},t+\delta)$; we then repeated the integration step, starting again from $\psi(\boldsymbol{r},t)$, but using $\frac{1}{2}[\psi(\boldsymbol{r},t) + \tilde{\psi}(\boldsymbol{r},t+\delta)]$ in the nonlinear term. In Fig. 1 we show a typical time evolution obtained from the integration of the GPE. We plotted here $N^{-1}\int |\psi(\boldsymbol{r},t)|^2\,\mathrm{d}y\,\mathrm{d}z$ as function of t and x. The initial wave function we started from has the form of Eq. (4), with $\sigma_i = 1$ and $\beta_i = 0$ for $i = 1,2,3$, i.e., fairly far from equilibrium.

The Gaussian wave function is not an exact steady-state solution for the GPE, as also stated in Ref. [13]. The small deviations from the actual stationary solution excite small-amplitude oscillations in the condensate distribution. We have spectrally analyzed the time dependence of the condensate widths along the three spatial directions, in order to derive the oscillation frequencies. This analysis has been done for different

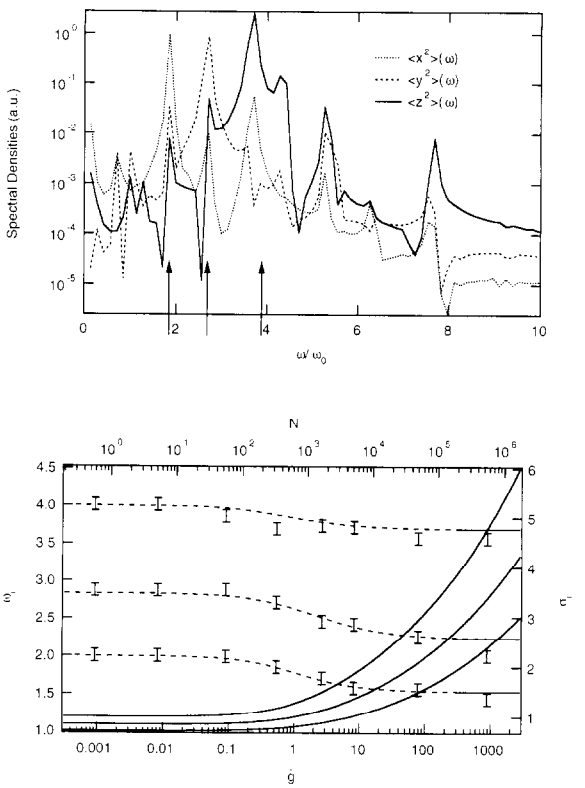

Fig. 2. Top: Typical spectral densities from the numerical integration of the GPE: we show the Fourier transform of the time evolution of the condensate widths along the three axes, for the Na case and $\tilde{g} = 0.664$. The arrows show the location of the eigenmode frequencies expected from the variational analysis. Bottom: Results for the variational calculation of the scaled oscillation frequencies ω_i, in units of ω_0 (dashed lines), and scaled widths σ_i, in units of a_0 (continuous lines), as a function of $\tilde{g}$ (lower scale) and N (upper scale). The horizontal segments on the right represent the hydrodynamic limits. The markers indicate the oscillation frequencies derived from numerical integration of the GPE. Triaxial TOP parameters as in Ref. [8] and scattering length $a = 2.75$ nm.

values of $\tilde{g}$, for both positive and negative scattering lengths. A typical spectral density is shown in Fig. 2 (top).

The general solution of Eq. (8) for the stationary state and of Eq. (9), the eigenvalue problem for the collective mode frequencies, was obtained numerically. This solution is shown in Fig. 2 (bottom), where the scaled widths σ_i of the stationary condensate wave-function, solid lines, and the normal mode frequencies ω_i, dashed lines, are shown as functions of the coupling strength $\tilde{g}$ in case of a positive scattering length a. Fig. 3 (top) shows the same quantities for

a negative scattering length a. On the top axes of the graphs in Figs. 2 (bottom) and 3 (top), the number N of atoms in the condensate is reported, for scattering lengths and trapping potential parameters fixed to the values listed below. The markers in Figs. 2 and 3 represent the mode frequencies calculated from the numerical solution of the GPE. The results in Fig. 2 are obtained for parameters corresponding to the triaxially anisotropic trap used in the experiment in Ref. [8], performed at NIST on Na atoms, e.g., $\omega_0 = 2\pi \times 234$ s^{-1}, $\lambda_1 = 1$, $\lambda_2 = \sqrt{2}$ and $\lambda_3 = 2$. The Na scattering length $a = 2.75$ nm is used in the calculation. The equilibrium solutions for the condensate widths σ_i are increasing functions of the condensate number N and, asymptotically, scale as $N^{1/5}$. The mode frequencies decrease with N monotonically from the non-interacting values to the asymptotic values, indicated in the figure by the solid horizontal segments.

Fig. 3 (top) shows the solution for a negative scattering length $a = -1.4$ nm, appropriate for ^{7}Li atoms. The parameters characterizing the trapping potential are the same as in Fig. 2. For small condensate numbers we recover again the non-interacting limit. With increasing N, the atom–atom interaction strongly modifies the dynamics of the condensate, in a different way with respect to the case of positive scattering length. Notice the different horizontal scales in Figs. 2 and 3. It is worth noting that the variational formalism, being applicable for any condensate number N, makes it possible to investigate the case of negative scattering lengths. In this case, the large N limit of the Thomas–Fermi approximation and the hydrodynamic approach do not apply, because the number of condensed atoms cannot exceed a critical value [4]. For negative coupling constant $\tilde{g}$, Eqs. (8) present either two solutions for the stationary width σ_i of the condensate along each direction, or no solution, depending on the absolute value of $\tilde{g}$. This is shown in Fig. 3, where, for each σ_i, a two-branched solution is displayed (solid lines). The upper and lower branches of the σ_i curves correspond to the stable and the unstable solution, respectively. As functions of $|\tilde{g}|$, the stable stationary widths shrink, while the unstable ones, originating from zero as limit for $|\tilde{g}| \to 0$, increase. The two branches of each σ_i solution merge at a critical value of the coupling strength. Beyond this value, no solution to Eqs. (8) exists. The dashed lines in Fig. 3 show the frequencies of the collective mo-

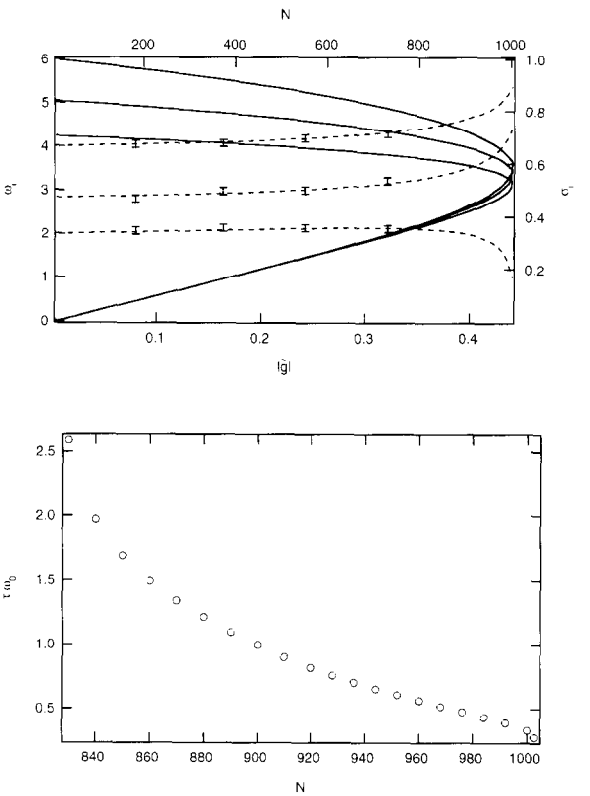

Fig. 3. Top: As in Fig. 2, except scattering length $a = -1.4$ nm. Bottom: time before we observe the condensate collapse, as a function of N, for the same parameters of the top figure. The initial wave function has the form of Eq. (4), with the σ_i equal to the variational ones, and $\beta_i = 0$.

tion around the stable solution. At the critical point, the two highest frequencies diverge and the lowest one falls to zero. Similar results have been obtained in Ref. [10] for cylindrically symmetric condensates. This theoretical results agree well with the numerical integration of the GPE.

However, in the case of negative scattering lengths the collapse of the condensate implies that the GPE can be numerically integrated only until the collapse takes place. As the number of particles in the condensate increases and approaches the critical value, the lifetime of the condensate decreases and, eventually, becomes so short that we can no longer observe any oscillatory dynamics. For the Li parameters, the collapse lifetime is shown in Fig. 3 as function of N, for N approaching the critical value.

In conclusion, we have performed an analysis of the dynamics of a Bose–Einstein condensate trapped

in a triaxially asymmetric potential. Condensation was achieved at NIST in a fully asymmetric TOP trap [8], while a specific study of the condensate dynamics in such a geometry was lacking. At present, no experimental data concerning the collective motion of the condensate are available from the NIST experiment. Our predictions might be confirmed by forthcoming experimental results. Within the different point of view started by Dalfovo et al. [14], the study of the nonlinear coupling between the condensate modes provides a stronger test of the condensate characteristics. Moreover, nonlinear processes could be useful to perform nonlinear spectroscopy or nonlinear optics in the condensate. As is well known in the framework of nonlinear dynamics, more complex scenarios are produced when the number of degrees of freedom is increased, as in the $(3+1)$-dimensional evolution in a triaxial magnetic trap.

This project was supported by the Italian INFM through a PRA project on Bose–Einstein Condensation and by the CNR through a Progetto Integrato. The authors wish to thank L. Reatto for a careful reading of the manuscript.

References

[1] M.H. Anderson, J.R. Ensher, M.R. Matthews, C.E. Wieman, E.A. Cornell, Science 269 (1995) 198.

[2] C.C. Bradley, C.A. Sackett, J.J. Tollett, R.H. Hulet, Phys. Rev. Lett. 75 (1995) 1687.

[3] K.B. Davis, M.O. Mewes, M.R. Andrews, N.J. van Druten, D.S. Durfee, D.M. Kurn, W. Ketterle, Phys. Rev. Lett. 75 (1995) 3969.

[4] F. Dalfovo, S. Giorgini, L.P. Pitaevskii, S. Stringari, Rev. Mod. Phys., in press.

[5] M.-O. Mewes, M.R. Andrews, N.J. van Druten, D.M. Kurn, D.S. Durfee, C.G. Townsend, W. Ketterle, Phys. Rev. Lett. 77 (1996) 988.

[6] D.S. Jin, J.R. Ensher, M.R. Matthews, C.E. Wieman, E. Cornell, Phys. Rev. Lett. 77 (1996) 420;
D.S. Jin, M.R. Matthews, J.R. Ensher, C.E. Wieman, E. Cornell, Phys. Rev. Lett. 78 (1997) 764.

[7] D.M. Stamper-Kurn, H.-J. Miesner, S. Inouye, M.R. Andrews, W. Ketterle, Phys. Rev. Lett. 81 (1998) 500.

[8] R. Lutwak, L. Deng, E. Hagley, M. Kozuma, J. Wen, K. Helmerson, S. Rolston, W.D. Philips, J. Phys. B, submitted.

[9] D. Anderson, Phys. Rev. A 27 (1983) 3135;
M. Desaix, D. Anderson, M. Lisak, J. Opt. Soc. Am. B 8 (1991) 2082.

[10] V.M. Pérez-Garcia, H. Michinel, J.I. Cirac, M. Lewenstein, P. Zoller, Phys. Rev. Lett. 77 (1996) 5320; Phys. Rev. A 56 (1997) 1424.

[11] A. Parola, L. Salasnich, L. Reatto, Phys. Rev. A 57 (1998) R3180.

[12] Y. Castin, R. Dum, Phys. Rev. Lett. 77 (1996) 5315;
Yu. Kagan, E.L. Surkov, G.V. Shlyapnikov, Phys. Rev. A 54 (1996) R1753.

[13] K.G. Singh, D.S. Rokhsar, Phys. Rev. Lett. 77 (1996) 1667.

[14] F. Dalfovo, C. Minniti, L.P. Pitaevskii, Phys. Rev. A 56 (1997) 4855;
F. Dalfovo, C. Minniti, S. Stringari, L. Pitaevskii, Phys. Lett. A 227 (1997) 259.